AN ABSTRACT OF THE THESIS OF

Casey P. Kernan for the degree of Honors Baccalaureate of Science in Bioresource Research presented on May 25th, 2012. Title: DNA Mismatch Repair-Dependent Suppression of Genotoxicity of Benzo[a]pyrene Diol Epoxide.

Abstract approved:

_____

Andrew Buermeyer

DNA mismatch repair (MMR) plays an important role in preserving genomic stability and reducing cancer risk. Environmental exposures to polycyclic aromatic hydrocarbons (PAHs) are believed to contribute significantly to carcinogenesis. PAHs are found in food, air, water and soil and upon bioactivation can form diol epoxides which are electrophilic in nature and can adduct to DNA, creating bulky PAH-DNA lesions. Preliminary data in the Buermeyer laboratory demonstrated that mutations induced by benzo[a]pyrene diol epoxide (BPDE) occur at higher rates in MLH1-deficient HCT 116+Ch2 cell line (30±7 mutations per 100 nM BPDE) versus a genetically matched MLH1-proficient line HCT 116+Ch3 cell line (10±4 mutations per 100 nM BPDE). I hypothesized that the role for MMR in suppressing mutation is a phenomenon generalizable to other cell lines. I measured BPDE-induced mutation rates in the parent cell line HCT 116, and in another genetically matched MSH6-proficient and -deficient set. I found an induced mutation rate of 30±5 mutations per 100 nM BPDE using HCT 116 cells, not significantly different from the induced mutation rate with HCT 116+Ch2 cells. In addition, we characterized mutants from HCT 116+Ch2 clones and identified 25 individual mutations with the predominance of G→T transversions.

Key Words: DNA Mismatch Repair, Polycyclic Aromatic Hydrocarbons, Cancer

Corresponding Email Address: kernanc@onid.orst.edu

DNA Mismatch Repair-Dependent Suppression of Genotoxicity

of Benzo[a]pyrene Diol Epoxide.

by

Casey Kernan

A PROJECT

submitted to

Oregon State University

University Honors College

In partial fulfillment of

the requirements for the

degree of

Honors Baccalaureate of Science in Bioresource Research (Honors Associate)

Presented May 25th, 2012

Commencement June 2012

<u>Honors Baccalaureate of Science in Bioresource Research</u> project of <u>Casey Kernan</u>
presented on <u>May 25th, 2012.</u>

APPROVED:

_____

Mentor, representing Environmental and Molecular Toxicology

_____

Committee Member, representing Environmental and Molecular Toxicology

_____

Chair, Department of Bioresource Research

_____

Dean, University Honors College

I understand that my project will become part of the permanent collection of Oregon

State University, University Honors College. My signature below authorizes release of

my project to any reader upon request.

_____

Casey Kernan, Author

Acknowledgments

I wish to thank my mentor, Dr. Andrew Buermeyer for his patience and continued support during this project. Thanks are due to Vidya Shalks who helped with the initial stages of the project, in particular with the analysis of HPRT mutations, and to the serving committee members, Dr. John Hays and Dr. Katherine Fields. Additional thanks to Dr. Kevin Ahern, the Howard Hughes Medical Institute and the Environmental Health Science Center for providing funding and support. I would like to acknowledge the other undergraduates in the lab for their help throughout many stages of the project and for making the lab a fun and enjoyable environment to work in. Finally, I would like to acknowledge my family for their tremendous support and encouragement throughout my undergraduate experience.

TABLE OF CONTENTS

Introduction

Materials and Methods

Results and Discussion

LIST OF FIGURES

LIST OF TABLES

LIST OF ABBREVIATIONS

6-TG	6-Thioguanine
6-TG^R	6-Thioguanine resistant
AHR	Aryl hydrocarbon receptor
ARNT	Aryl hydrocarbon nuclear translocator
BPDE	Benzo[a]pyrene diol epoxide
CRC	Colorectal cancer
CYPs	Cytochrome P450
HAT	Hypoxanthine Aminopterin Thymidine
HNPCC	Heriditary non-polyposis colorectal cancer
HPRT	Hypoxanthine-guanine phosphoribosyl transferase
IDL	Insertion/deletion loops
MF	Mutant frequency
MMR	Mismatch Repair
MSI	Microsatellite Instability
PAH	Polycyclic aromatic hydrocarbon
PE	Plating efficiency
XRE	Xenobiotic response element

Environmental Carcinogens

A number of cellular pathways, processes and environmental genotoxins interact to influence individual susceptibility and risk of cancer development. Environmental carcinogens are ubiquitous in nature and human exposure is unavoidable. In 2010, the American Cancer Society estimated that the lifetime risk of cancer development among males is nearly one in two and one in three for females. During 1775, Sir Percivall Potts, an English surgeon, was the first to observe an association between chimney sweeps and a higher incidence of scrotal cancers. These investigations marked the first identified occupational link to cancer and have had a profound impact on the science of epidemiology and the study of environmental carcinogens. Nearly a century later (1875) workers in the coal tar industry were developing skin cancers at an elevated rate and by the 1900s it was recognized that soot, coal, tar and pitch are carcinogenic to man. In 1930, one of the chemicals responsible for inducing many of these occupational cancers was isolated and determined to be benzo[a]pyrene (B[A]P) (Gabrieli, 2010). More recently, 100's of similar chemicals called polycyclic aromatic hydrocarbons (PAH) have been studied, with B[A]P being of main focus in many of the studies.

PAH Exposure

Large planar aromatic PAHs result from the incomplete combustion of organic material. Ubiquitous in nature, these environmental pollutants are found in an array of settings. The major anthropogenic atmospheric emission sources of PAHs include biomass burning, coal and petroleum combustion, and coke and metal production (Zhang,

2009). Natural events such as forest fires and volcanic eruptions contribute to levels of PAHs in the air, soil and environment. Abundance and distribution of PAHs in different countries largely depends on population density, energy production strategies, vegetation cover, consumer good production and level of development. Generally, countries with greater population density and industrialization have considerably higher PAH emissions. In 2004, the primary sources of PAHs were from biofuel (56.7%), wildfire (17.0%) and consumer product usage (6.9%) with China, India and the United States being the top three countries with the highest PAH emissions: 114 giga grams per year (Gg y^{-1}), 90 Gg y^{-1} and 32 Gg y^{-1}, respectively (Zhang, 2009).

Human exposures to PAHs can result from inhalation, ingestion and uptake through the skin, while exposure through the diet seems to be the predominate form. Measurable levels of PAHs have been found in uncooked foods, leafy vegetables, cooked meats and cigarette smoke. Processed or smoke-cured meats and fish, meats cooked over an open flame and charred foods are often higher in PAHs. Studies in European countries, aimed to address daily intakes of PAHs among individuals have estimated levels between 3.7 μg to 17 μg of PAHs per day. In 1987 the Food and Agriculture Organization (FAO) and World Health Organization (WHO) declared that amounts of B[a]P, a common PAH, should not exceed 10 ppb in foods; however, some barbecued meats have contained levels reaching 30 ppb of B[A]P (Phillips, 1999). Over 100 other PAHs have been characterized. The Environmental Protection Agency (EPA) has identified 16 as 'priority pollutants', 15 of which have been reported to be the most carcinogenic, cytotoxic and mutagenic: benzo(*a*)anthracene, cyclopenta(*c,d*)pyrene, chrysene,5-methylchrysene, benzo(*b*)fluoranthene,

benzo(*j*)fluoranthene, benzo(*k*)fluoranthene, benzo(*a*)pyrene, indeno(1,2,3-*c,d*)pyrene,

dibenzo(*a,h*)anthracene, benzo(*g,h,i*)perylene, dibenzo*(a,l)*pyrene, dibenzo(*a,e*)pyrene,

dibenzo(*a,i*)pyrene, dibenzo(*a,h*)pyrene (Figure 1).
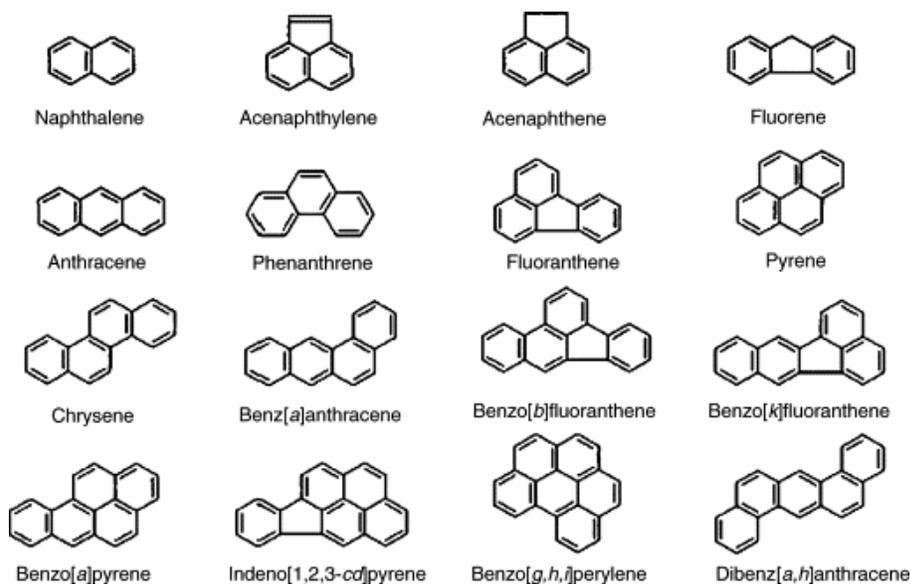
Figure 1. The chemical structure of the 16 EPA priority PAHs. (Figure from Anyakora 2005)

PAH Characteristics and Metabolism

The International Agency for Research on Cancer (IARC) classifies B[a]P as a group 1

carcinogen, indicating it is carcinogenic to humans. The nonpolar structure of B[a]P can

pass easily through cell membranes where the toxin is bioactivated and metabolized by

cytochrome P450 enzymes, predominately CYP1A1 and CYP1B1 enzymes. Further

metabolism by epoxide hydrolase, transforms B[a]P into a highly reactive diol epoxide

(Baird 2005). The large family of cytochrome P450 (CYPs) enzymes are substrate-

inducible and are responsible for the metabolism of a number of drugs, xenobiotics and

steroids. Exposure to PAHs result in induction of CYP enzymes via the aryl hydrocarbon

receptor (AHR), which binds planar PAHs, such as B[a]P, more readily than compounds

with distorted planarity. The cytosolic AHR receptor dimerizes with the aryl

hydrocarbon nuclear translocator (ARNT), enters the nucleus and interacts with genes

containing a xenobiotic response element (XRE), resulting in induced or upregulated

expression of proteins involved in xenobiotic detoxification (Baird 2005). Due to the

ability of PAHs to act as AHR receptor agonists, induction of carcinogen-metabolizing

CYP enzymes is increased upon PAH exposure. CYP's first act on PAH's by adding an

epoxide group which can then be either detoxified or bioactivated by conversion to a

dihydrodiol by epoxide hydrolase. B[a]P is metabolically activated to benzo[a]pyrene

diol epoxide (BPDE) and can form four metabolites in both *syn* and *anti* enantiomer pairs

(Figure 2).
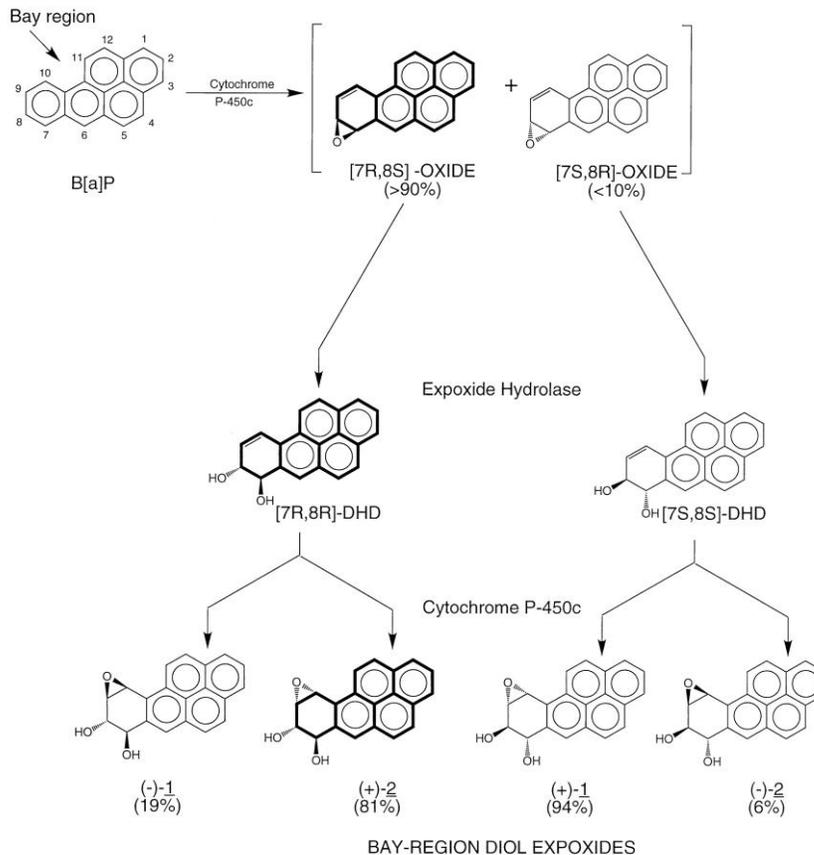
Figure 2. Regio- and stereoselectivity of CYP1A and epoxide hydrolase in the formation of bay-region diol epoxides of benzo[a]pyrene (Figure from Thakker 1988)

Due to the electrophilic nature of BPDE, it adducts preferentially to negatively charged

DNA, creating a bulky PAH-DNA adduct that is often replicated incorrectly resulting in

genetic mutation. While a number of metabolites of B[a]P exist, metabolic activation to

anti BPDE is generally the most carcinogenic metabolite in animal studies (Baird, 2005).

The metabolite, BPDE is a potent genotoxin that adducts to guanine bases and to

a lesser extent, adenine and cytosine. Nucleotide excision repair (NER) removes bulky

lesions such as B[a]P -DNA adducts. When not repaired by NER, such adducts impair

the progress of the replication fork. This may lead to translesion synthesis (TLS,)

requiring bypass by different polymerases that have varying efficiencies and fidelities

(Lagerquist, 2008). We hypothesize that the exposure of PAHs such as B[a]P, coupled

with an individual's inability to suppress mutations efficiently via various evolutionarily

conserved DNA repair pathways, increases susceptibility and risk of developing cancer.

MMR Mechanisms and Machinery

Among DNA repair pathways, mismatch repair (MMR) corrects mismatched base

pairs and small insertion/deletion loops (IDLs) caused by DNA replication errors that

escape the proofreading activities of replicating polymerases. MMR improves the

fidelity of DNA replication by several orders of magnitude and thereby contributes to

genome stability. The fundamental mechanisms and associated proteins are highly

conserved in all organisms, from bacteria to humans. While two models have been

elucidated, one employed by eukaryotes and another specific to *E. coli*, less is known

about the more involved eukaryotic processes. A successful MMR pathway must

efficiently recognize base-base mismatches and IDL's and direct the repair machinery to the newly synthesized DNA strand containing the erroneous genetic information (Jiricny, 2006).

In *E. coli*, the primary proteins responsible for mediating mismatch repair include MutS, MutL and MutH. The recognition of biosynthetic errors is accomplished by a MutS homodimer, which then recruits a homodimer of MutL. The ATP-dependent formation of this ternary complex activates the endonuclease activity of MutH which nicks hemimethylated DNA on the unmethylated strand at a GATC site (Jiricny, 2006). The error-containing DNA strand is removed by the cooperative functions of DNA helicases, such as UvrD, the exonucleases RecJ and ExoI, and the single-stranded DNA-binding protein SSB. SSB functions to prevent the strands from reannealing back into the double helix (Fukui, 2010). Once the mismatch has been removed, the exonucleolytic degradation ceases and the resulting gap is then filled by DNA polymerase III and repair is completed when DNA ligase seals the remaining nick (Jiricny, 2006).

The MMR mechanism in eukaryotes is more complex than in *E. coli* and involves the participation of heterodimers for the core proteins that have specific known and unknown functions (Table 1).

Complex	Components	Function	References
MutSα	MSH2, MSH6	Recognition of base–base mismatches and small IDLs	17–19,30
MutSβ	MSH2, MSH3	Recognition of IDLs	19,25
MutLα	MLH1, PMS2	Forms a ternary complex with mismatch DNA and MutSα; increases discrimination between heteroduplexes and homoduplexes; also functions in meiotic recombination	43,65,71,73
MutLβ	MLH1, PMS1	Unknown	44
MutLγ	MLH1, MLH3	Primary function in meiotic recombination; backup for MutLα in the repair of base–base mismatches and small IDLs	45,46,110

Table 1 | Human MutS and MutL homologue complexes that are involved in mismatch repair

IDL, insertion/deletion loop; MLH, MutL homologue; MSH, MutS homologue; PMS, post-meiotic segregation protein.

Table 1: Human MutS and MutL homologue complexes involved in mismatch repair (Table from Jiricny, 2006)

Of the five MutS homologues (MSH) that have been identified in human cells, MSH2, MSH3 and MSH6 participate in MMR as MutSα (MSH2·MSH6) and MutSβ (MSH2·MSH3). MutSα is responsible for initiating the repair of base-base mismatches and small IDLs while MutSβ deals predominantly with the recognition of IDLs (Jiricny, 2006). The MutS complexes associate with the DNA, recruiting another heterodimeric complex comprised of MutL homologues. The human homologue of prokaryotic MutL has three forms designated as MutLα, MutLβ and MutLγ. The MutLα complex is made of two subunits MLH1 and PMS2, the MutLβ heterodimer is made of MLH1 and PMS1, while MutLγ is made of MLH1 and MLH3. MutLα acts as the molecular matchmaker, coordinating events in mismatch repair (Cannavo, 2005). The interaction between the MutS and MutL heterodimeric complexes is essential for activation of successive MMR steps (Wang, 2006).

The MutLα (MLH1·PMS2) heterodimer harbors a latent endonuclease activity that nicks the discontinuous strand of the mismatched duplex either 3' or 5' from the site of the mismatch. Following MutLα endonuclease activity, EXO1 directs exonuclease

activity 5'-3', removing the DNA segment spanning the mismatch (Figure 3). The single strands are stabilized by replication protein A (RPA), an analog to SSB in prokaryotic MMR (Fukui, 2010).

5′

3′

EXO1-dependent
excision reaction

(a) 5′-nicked
heteroduplex

(b) 3′-nicked
heteroduplex
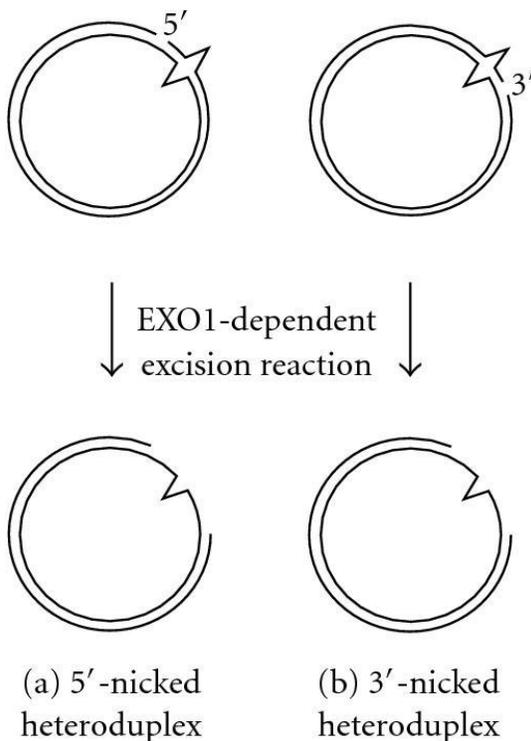
Figure 3. Bidirectionality of eukaryotic MMR. (Fukui, 2010)

Additional machinery and factors are required for MMR and subsequent DNA replication to operate efficiently, including the homotrimeric proliferating cell nuclear antigen (PCNA). This sliding clamp is loaded onto the 3' terminus of an Oakazaki fragment or onto the 3' end of the leading strand by replication factor C (RFC). Once loaded, it associates with DNA polymerase δ, improving overall processivity. This complex fills the gap and DNA ligase I seals the remaining nick (Jiricny, 2006).

MMR Deficiency and Lynch Syndrome

The association of MMR deficiency and carcinogenesis was first recognized in the study of Lynch Syndrome, also known as hereditary nonpolyposis colorectal cancer (HNPCC) (Papadopoulos *et al*, 1994). Individuals with this autosomal dominant genetic condition inherit a germline mutation in one or more of the four essential MMR genes: hMLH1·hPMS2 (MutLα) and hMSH2·hMSH6 (MutSα), impairing DNA MMR and placing them at a high risk of developing early-onset colon cancer. Individuals with mutations in genes necessary for MMR also have an increased risk of certain extra-colonic cancers, including tumors of the endometrium, stomach, small bowel, ovary, hepatobilliary tract, renal pelvis, and ureter (Pino, 2009).

Nearly 50% of the Western population develops a colorectal tumor by the age of 70, and in about 1 in 10 of these individuals, malignancy ensues as progression of the tumor occurs at an elevated rate (Kinzler, 1996). As a result colorectal cancer is the second leading cause of cancer-associated deaths in the United States, second to lung cancer. Lynch Syndrome accounts for 2%-4% of the total colorectal cancers in the Western world (Lynch et. al., 1996). Tumors that develop due to defects in MMR often exhibit alterations in repetitive DNA sequences known as microsatellites. This so-called microsatellite instability (MSI) is defined as an elevated rate of insertion/deletion mutations in microsatellites. MSI can be identified in greater than 90% of colorectal cancers that arise in individuals with Lynch Syndrome, whereas in sporadic colorectal cancer it occurs in 15% of cases, typically from silencing of the MLH1 gene by promoter hypermethylation (Pino, 2009). A combination of MSI and immunohistochemical

analyses (IHC) testing of colorectal adenomas is a sensitive screen for the detection of Lynch Syndrome (Pino, 2009).

Progression of cancerous tumors is associated with a concept coined the mutator phenotype. Believed to be a driver of cancer tumorigenesis, the mutator phenotype concept in cancer was initially formulated based on mutations in DNA polymerases that render them error-prone and mutations in enzymes involved in DNA repair that decrease the ability of cells to remove potentially mutagenic DNA lesions (Loeb, 1974). It is estimated that each cell undergoes >20,000 DNA damaging events and >10,000 replication errors per cell per day (Loeb, 2011). Over time during the development of a cancer mutations accumulate, activating onco-genes and rendering suppressor genes inactive, thereby allowing the tumor to develop a clonal advantage as it can become resistant to chemotherapeutic drugs and avoid apoptosis. Evidence for the importance of a mutator phenotype in the development of cancers has been demonstrated in rodent models. Mice with mutations inactivating MMR genes or the proof-reading functions of the replicative DNA polymerases Polδ and Polε have an increased incidence of spontaneous cancer (Loeb, 2011). Even in the absence of environmental stress, MMR-deficient rodents in these studies show elevated spontaneous tumorigenesis and MSI.

Due to the complex nature of cancer cells, it is difficult to design efficacious drugs that effectively limit the progression of a tumour. However, identifying resistance that develops in certain cancer cell lines is a step towards personalized chemotherapy. Understanding how certain mutations lead to clonal resistance and designing effective chemotherapy regimens will provide a more effective and less toxic therapy for individual patients.

Overview of Study

Defects in various cellular pathways and exposure to environmental carcinogens interact to influence an individual's risk of developing cancer. Using MMR-proficient and -deficient colon cancer cell lines we sought to confirm preliminary data in the Buermeyer lab suggesting that MMR is a key pathway for reducing deleterious mutations induced upon PAH exposure. We hypothesized that the role of MMR in suppressing mutation is a phenomenon generalizable to other cell lines and other PAHs. My results are consistent with the hypothesis that MLH1-deficient cells show significantly elevated rates of mutation induced by BPDE. Preliminary characterization of the specific mutations induced in MLH1-deficient cells is consistent with BPDE-adduction to guanine bases. While addressing this hypothesis we encountered a number of technical issues with the assay and worked toward correcting them. Initial investigations of use of exogenous metabolizing extracts identified a significant toxicity and point to a need for further optimization.

Materials and Methods

Cell Lines

Adherent human colon carcinoma cell lines, HCT 116, HCT 116+Ch2, HCT 116+Ch3, DLD1 and DLD1+Ch2, were used. The HCT 116 and DLD1 chromosome-transfer cell lines (chromosomes 2 and 3, respectively) were derived by microcell-mediated chromosomal transfer (CR Boland and TA Kunkel) and selected using G418 Sulfate Medium (IMDM Medium + 400µg[active]/mL G418 Sulfate). For routine maintenance of all cell lines, cells were cultured sub-confluently under sterile conditions in Iscove's Modified Dulbecco's Medium (IMDM, supplemented with 4.00 mM L-glutamine, 25 mM HEPES buffer, sodium pyruvate 1mM) (Invitrogen) supplemented with 10% fetal bovine serum (FBS, HyClone) and penicillin streptomycin (1x) at 37ºC in 5% CO_2 humidified incubators. Subculture was performed by use of trypsin (Gibco) solution.

Measurement of PAH-Induced Mutations in HPRT

PAH-induced mutations were measured using the hypoxanthine phosphoribosyl transferase (*HPRT*) gene. To measure mutations induced by PAH exposure, cell lines were first cleared of any preexisting HPRT mutants by growth in a selective HAT (hypoxanthine aminopterin thymidine) medium. Cells were maintained in HAT Medium (2X hypoxanthine, aminopterin, thymidine) (Cellgro) for five 1:5 passages. HAT

medium forces cells to rely on salvage pathways including HPRT function to synthesize nucleotide precursors, and therefore selectively kills HPRT-deficient cells.

Following removal of HPRT mutants, cells were plated at density of 0.6×10^6 cells in 10cm dishes and allowed to recover overnight. Racemic (+/-) BPDE (Midwest Research Institute) was resuspended in anhydrous dimethyl sulfoxide (DMSO) (Sigma, St Louis, MO) at concentrations of 200-250μM immediately prior to use. Chemical exposures were performed in serum-free medium (IMDM). Cells were exposed to BPDE (generally $\geq$ 1:1000 x dilutions of BPDE stock) for 1 hour at 37 °C, after which BPDE-containing medium was aspirated, plates were rinsed with PBS and fresh medium (IMDM + 10% FBS) was replaced.

Following BPDE exposure, growth medium was exchanged and surviving cells were maintained subconfluently for up to 8 days to allow for phenotypic expression of HPRT mutants. To measure HPRT-mutant frequencies, cells were harvested and plated at a density of 0.135×10^6 cells per 30 cm dish in 6-thioguanine selective (6-TG) medium (IMDM growth medium with 40 μM 6-TG) and incubated 2 weeks to allow growth of 6-TG[R] colonies. In parallel, 300 cells were plated in IMDM Medium with no 6-TG and allowed 8-12 days for colony development to determine a plating efficiency for each culture (PE = number of colonies per 300 cells plated). Each culture received fresh medium 6-8 days after initial plating. Ultimately, colonies were visualized by methylene blue fixation and staining, and 6-TG[R] colonies were visually counted.

PEs and colony counts were used to calculate mutant frequency according to the following equation:

$$MF = (\text{total number of 6-TG}^R)/(PE \times \text{total number of cells plated})$$

MF = mutant frequency
6-TG^R = 6-thioguanine resistant colonies
PE = plating efficiency

Benzo[a]pyrene + S9 Mix

Induction of mutation with B[a]P was similar to BPDE described above, with the addition of S9 extract described below. HCT 116+Ch2 and HCT 116+Ch3 cell lines were cleared of preexisting HPRT mutations in HAT medium, harvested and plated at a density of 1.0×10^6 cells. The following day, each plate was aspirated, rinsed with 5 ml of PBS and 4 ml of serum-free IMDM medium was added. B[a]P (stock solution in DMS0 was 2.28 mg/mL) was a generous gift from the Kim Anderson laboratory and the following concentrations were used: 0, 0.57, 1.14, 2.28 μg/mL. S9 protein and NADPH-regenerating system reagents were purchased from Moltox (Boone, NC). NADPH-regenerating system B, consisting of lyophilized NADPH was thawed at room temperature and reconstituted with 1 mL of cold regenerating system A (Glucose-6-Phosphate, MgCl$_2$ in 0.1 M phosphate buffer, Ph 7.4) and the mix was transferred back to regenerating system A vial and stored on ice. To complete the S9 mix, 5 mL of S9 liver protein (40.8 mg/mL) from aroclor-1254-induced Sprague Dawley rats was added to 20 mL of regenerating system A to give a final 10% S9 Mix. Immediately after preparation,

1 mL of 10% S9 Mix was added to each plate. The final concentrations of all

constituents of the S9 mix is one-fifth of the total concentration of medium, since 1 mL

of this mix is added to 4 mL of serum-free medium for the treatment. After the addition

of the above noted stock concentrations of B[a]P, each independent culture was exposed

in incubators for 3 hours at 37 ºC. The S9 Mix-containing media was aspirated, plates

were rinsed twice with PBS and IMDM medium supplemented with 10% fetal bovine

serum (FBS, HyClone) and penicillin streptomycin (100x) was added. Cells were

maintained and subcultured allowing for phenotypic expression.

Cytotoxicity

The cytotoxic response to BPDE or B[a]P + S9 exposure was determined for cell

lines by colony-forming ability. Twenty-four hours following PAH exposure, cells were

harvested with trypsin, and live cells were counted using a hemocytometer loaded with

10µl of cell culture + Trypan Blue (Sigma) in a 1:1 ratio. 300-500 cells were plated in 10

cm dishes in duplicate for each dose. Colonies were allowed to grow for 12–14 days and

were visualized by staining with methylene blue.

HPRT Mutant Analysis

Individual 6-TG^R colonies were picked and isolated using trypsinized cloning

discs and expanded into 12 and then in 6 well dishes in IMDM+6-TG medium. Upon

confluency, cells were harvested, pelleted and frozen for subsequent analysis. RNA was

purified from cell pellets, using Quiagen RNeasy Mini Kit, following manufacturer's directions. RNA concentrations were determined by using a NanoDropND-1000 Spectrophotometer to measure absorbance at 260 nm. The samples were stored overnight at -20°C until further analysis.

First-strand cDNA was synthesized from purified RNA via reverse transcription using Invitrogen SuperScript III First-Strand-Synthesis System. Approximately 1,500 ng of RNA was combined in a 0.5 ml tube with 50 µM oligo(dT)$_{20}$, 50 ng/µl random hexamers, 10 mM dNTP mix and DEPC-treated water to give a final volume of 10 µl. Samples were incubated at 65° C for 5 min and then placed on ice for at least 1 minute. A cDNA synthesis mix prepared with 20 µl 10X RT buffer, 40 µl of 25 mM MgCl$_2$, 20 µl 0.1 M DTT, 10 µl RNaseOUT and 10 µl of SuperScript III RT. 10 µl of the cDNA synthesis mix was added to each RNA/primer mixture and centrifuged briefly followed by incubation for 10 min at 25°C and 50 min at 50°C. The reactions were terminated at 85°C for 5 min and chilled on ice. The reactions were collected by brief centrifugation and 1 µl of RNase H was added to each tube and incubated for 20 min at 37°C. First-strand cDNA products were stored at -20°C.

Amplification of cDNA was performed by an additional PCR step using Promega GoTaq Green Master Mix. Master Mix was thawed at room temperature, vortexed, and then spun briefly in a microcentrifuge to collect the material at the bottom of the tube. The PCR reaction mix for each sample was prepared containing 12.5 µl of GoTaq Green Master Mix, 2.5 µl of P3 forward primer (CCT GAG CAG TCA GCC CGC GC, 100 pmol/µl), 2.5 µl of P4 reverse primer (CAA TAG GAC TCC AGA TGT TT, 100 pmol/µl), 2 µl cDNA template and nuclease-free water to give a final reaction volume of

25 µl. Reactions were placed in a thermal cycler and after an initial 3 min incubation at

95°C, underwent 30 cycles at 95°C for 1 min, 55° C for 1.5 min, and 72°C for 1 min.

PCR products were stored at -20°C.

The PCR products were then cleaned with USB ExoSAP-IT to eliminate

unincorporated primers and dNTPs. Quantification of products was estimated visually

following agarose gel electrophoresis and comparison to mass standards. The identified

coding sequence of each individual clone was aligned to the wild-type human *HPRT* gene

to identify the specific mutation. Both forward and reverse electropherograms were used

to verify identified mutations.

Results and Discussion

Research Goals

DNA Mismatch Repair (MMR) plays an important role in the suppression of mutation induced by many different DNA-damaging agents. Understanding how MMR mediates the suppression of mutation induced by genotoxic environmental compounds may provide a more accurate evaluation of individual risk and susceptibility to developing cancer. Preliminary data in the Buermeyer lab demonstrated that BPDE-induced mutations occur at a higher rate in an MLH1-deficient cell line verse a genetically matched MLH1-proficient line, suggesting that MMR is a key pathway for reducing deleterious mutations, and therefore carcinogenesis, due to PAH exposure. If true, then the role for MMR in suppressing mutation should be a phenomenon generalizable to other MMR-deficient cell lines and other PAHs as well. Using colon cancer cell lines from different sources, deficient and proficient in *MLH1* and *MSH6* MMR genes, I sought to reproduce the preliminary results and evaluate the cytotoxic response, induced mutation rate and spectrum of mutations induced by the model PAH BPDE and the parent compound B[a]P. This study aimed to optimize the *HPRT* gene mutation assay with the use of MMR-proficient and MMR-deficient mammalian colon carcinoma cell lines, providing a powerful tool for studying the effects of other PAHs, as well as the complex mixtures of PAHs that humans might typically be exposed to. Results described herein do generally confirm the previous data, and identify a important, previously unappreciated technical aspect of genotoxicity studies using mutator cell lines.

I. Initial Hypothesis Test

Preliminary data produced in the Buermeyer laboratory suggested that MMR is a key pathway for reducing mutations induced by exposure to BPDE. The MLH1-deficient HCT 116+Ch2 cell line displayed higher BPDE-induced mutation rates (here defined as 6-TG^R mutants induced per unit dose of BPDE) relative to its genetically matched MLH1-proficient HCT 116+Ch3 cell line (Figure 4. Vidya Shalk and Andrew Buermeyer, unpublished data).
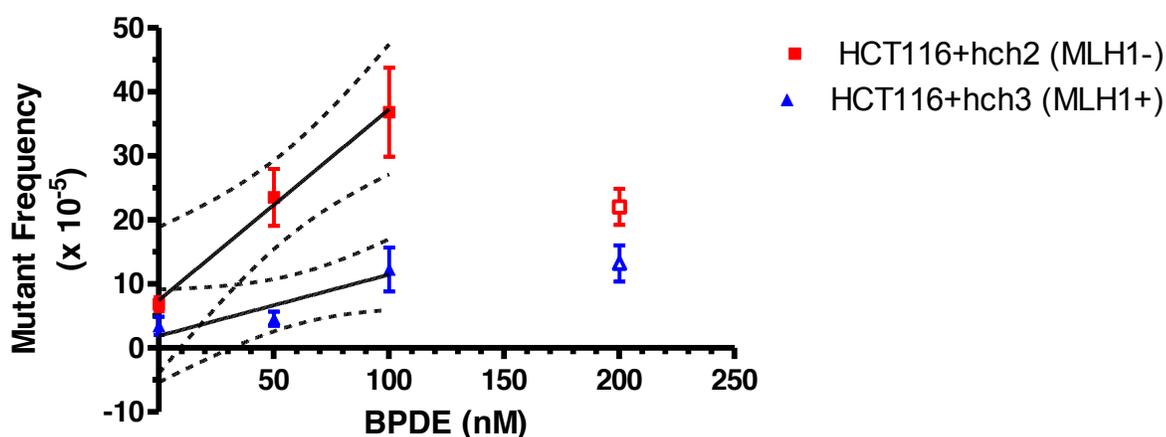
Figure 4. BPDE-induced 6-TG^R mutation rates in MLH1-proficient HCT 116+Ch3 (10±4 mutants per 100 nM BPDE; r^2 = 0.68) and MLH1-deficient HCT 116+Ch2 cell lines (30±7 mutants per 100 nM BPDE; r^2 = 0.42) (p = 0.036). Plotted is the linear regression of data from two independent experiments which were pooled. Dotted lines are the 95% confidence intervals for the linear regression.

While it appears that active MMR suppresses BPDE-induced mutations, an alternative explanation of these preliminary results is that the observed increased induced mutation rate is due to other genetic differences between the two lines, perhaps related to other genes on chromosome 2. If MMR plays a role in suppressing mutation, I

hypothesized that the observed phenomenon would be generalizable to other colon cancer cell lines, deficient and proficient in *MLH1* or other MMR genes. Using MMR-deficient HCT 116 (MLH1-), MMR-deficient DLD1 (MSH6-) and MMR-proficient DLD1+Ch 2 (MSH6+) cell lines I aimed to replicate the preliminary results and confirm the role for MMR in suppressing mutation induced by BPDE.

A. HCT 116 (MLH1-)

I first sought to confirm the preliminary findings using the parent cell line, HCT 116. The HCT 116+Ch3 and HCT 116+Ch2 cell lines were derived from the cell line, HCT 116, by a microcell- mediated chromosomal fusion to add the extra human chromosome. Chromosome 3 was added to make the parent cell line proficient in MMR, due to the functional copy of the wild-type *MLH1* gene residing on chromosome 3. The HCT 116+Ch2 cell line was also derived from the parent HCT 116 line and chromosome 2 was added as a control so that both cell lines were derived using similar manipulations, and could be grown in G418-selective medium. I exposed the parent HCT 116 cell line to BPDE and measured 6-TG^R mutant frequency at different doses of BPDE, with the expectation that we would see similar results to those with the HCT 116+Ch2 cell line (Figure 4).

The results, representing two experiments are presented in Figure 5. The apparent BPDE-induced mutation rate was 32±30 mutants per 100 nM BPDE, calculated as the slope of the linear regression, similar to previous measurements with the HCT 116+Ch2 cell line (30±7 mutants per 100 nM BPDE).
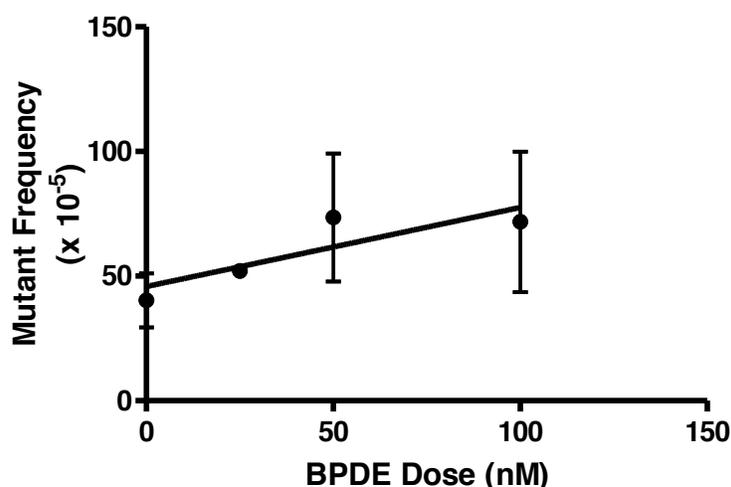
Figure 5. Initial measurement of BPDE-induced mutation in MLH1-deficient HCT 116 cells. Plotted is the mean plus standard error for 2-4 data points at each dose and the linear regression; ($r^2 = 0.09$). Data are pooled from 2 independent experiments.

While BPDE-mutant induction in this pooled data set (32 ± 3 mutants per 100 nM BPDE) closely resembled BPDE-mutant induction in previous experiments using HCT 116+Ch2 cells (30±7 mutants per 100 nM BPDE), the r^2 for the linear regression was low at 0.09, and likely due to the high spontaneous mutant frequencies at the zero dose. In both experiments, HCT 116 cells exhibited a high frequency of spontaneous mutation, as apparent in the 0 nM BPDE dose (MF=40 x10^{-5}). The mutation frequencies at the 0 and 50 nM BPDE dose were higher than anticipated (0 nM dose MF for HCT 116+Ch2 was 6.8x10^{-5}). The elevated spontaneous mutation made it difficult to ascertain the actual BPDE-induced mutation, suggesting that there may be a technical issue in these particular experiments. Plating efficiencies were rather low due to small colony formation. A low apparent plating efficiency can have the effect of artificially elevating the calculated mutant frequency. In addition to low plating efficiencies, ineffective HAT

treatment, differences in the cell lines and/or excessive phenotypic expression time may also contribute to an elevated calculated frequency of spontaneous mutation. The results from these two pooled experiments drew our attention to technical aspects of this assay that were underestimated in importance when using mutator cell lines.

Typically, cultures are given 8 days for phenotypic expression. This time period provides an opportunity for a number of population doublings following BPDE exposure, necessary to reduce the level of preexisting HPRT protein in a newly genetically mutant cell to levels that will not interfere with subsequent 6-TG selection. While there is some flexibility in the length of time for phenotypic expression using a non-mutator line due to the low rate of spontaneous mutation, the period of time before spontaneous mutations increase above detectable limits with a spontaneous mutator cell line is much shorter. Cultures that exhibit high rates of spontaneous mutation can acquire many mutations quickly, and reach levels that can interfere with the measurement of induced HPRT mutations (Figure 6). Defining the time period necessary and sufficient for phenotypic expression is therefore important in mutator cell lines.

.
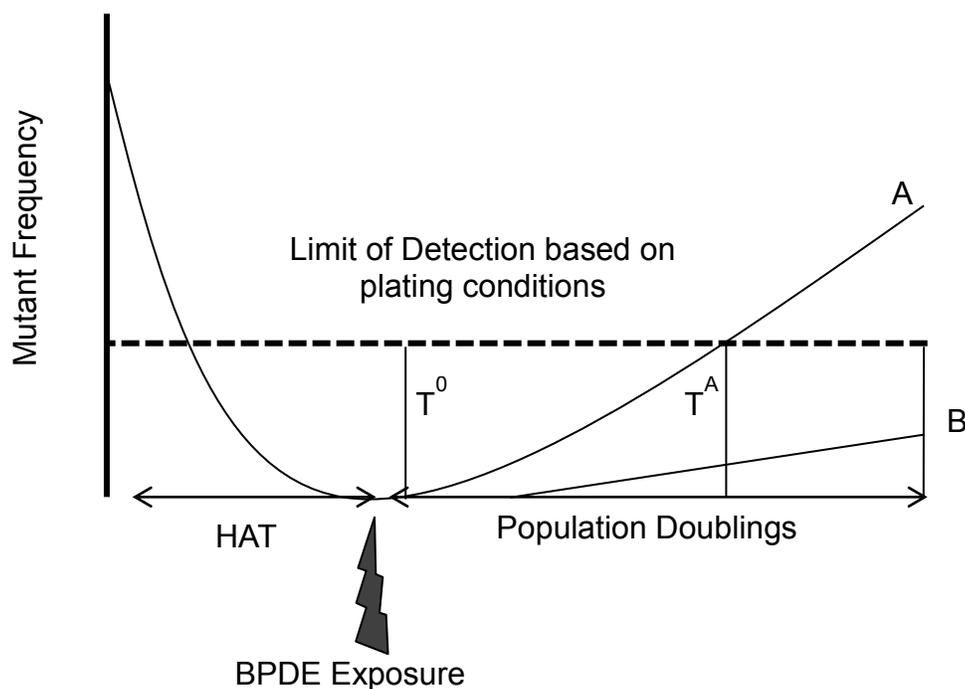
Figure 6. Spontaneous mutant induction in a mutator cell line. The accumulation of mutants with a mutator cell line (A) and normal cell line (B) following HAT treatment. T^0 corresponds to the start of phenotypic expression, following BPDE exposure. The effective or available window of time for phenotypic expression is significantly shorter with a spontaneous mutator cell line (T^A) vs. a normal cell line (T^B).

B. DLD1 (MSH6-) and DLD1+Ch2 (MSH6+)

To test the hypothesis that MMR-dependent suppression of mutation induced by BPDE is generalizable to cell lines proficient and deficient in other essential MMR proteins, I determined BPDE-induced cytotoxicity and rates of mutation using DLD1 (MSH6-) and DLD1+Ch2 (MSH6+) colon cancer cell lines (Figure 7).

A
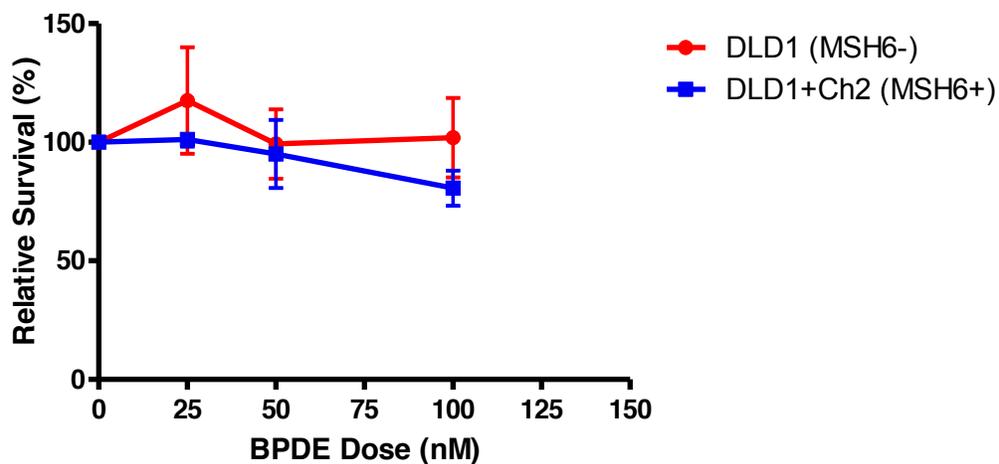
B
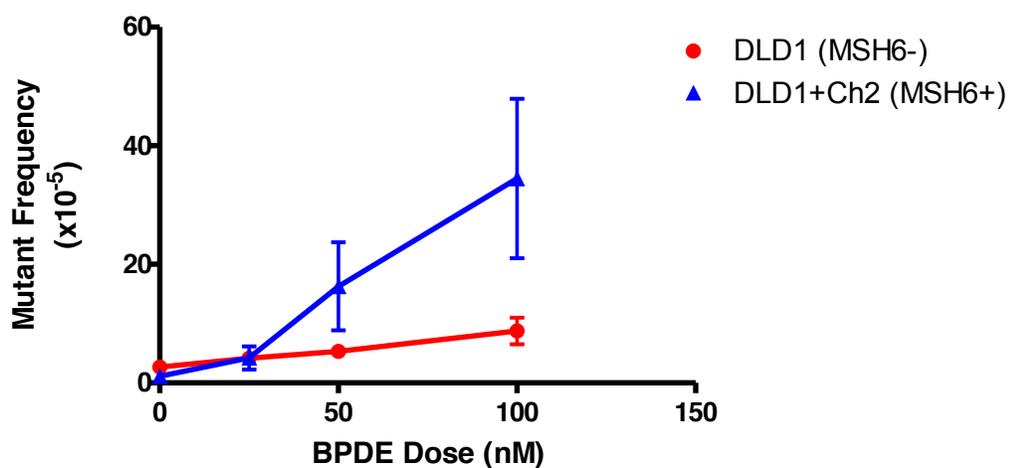
Figure 7. BPDE-induced cytotoxicity and BPDE-induced 6-TG^R mutation rates in DLD1 and DLD1+Ch2 cell lines. BPDE-induced cytotoxicity (A) and induced mutation rates (B) were measured as described in Materials and Methods. Plotted is mean plus standard error for 2 data points at each dose. Data from one experiment is included.

BPDE-induced cytotoxicity was minimal with no apparent differences between the two

cell lines. Spontaneous mutant frequencies were lower than the previous experiment,

more consistent with expectations. Surprisingly, the MSH6-deficient DLD1 cell line showed lower rates of induced mutation (6±1 mutations per 100 nM BPDE, r squared = 0.7695) compared to the MMR-proficient DLD1+Ch2 line (35±9 mutations per 100 nM BPDE, r squared = 0.7226). The high rate of induced mutation in the MSH6-proficient line (DLD1+Ch2) resembled results previously seen with MLH1-deficient HCT 116+Ch2 cell line (30±7 mutations per 100 nM BPDE). The explanation for such unexpected results is not clear, however low plating efficiencies were measured for the DLD1+Ch2 cell line versus the DLD1 cells (Figure 8). As noted in the previous section, low apparent plating efficiencies can have an effect of artificially elevating calculated mutant frequencies.
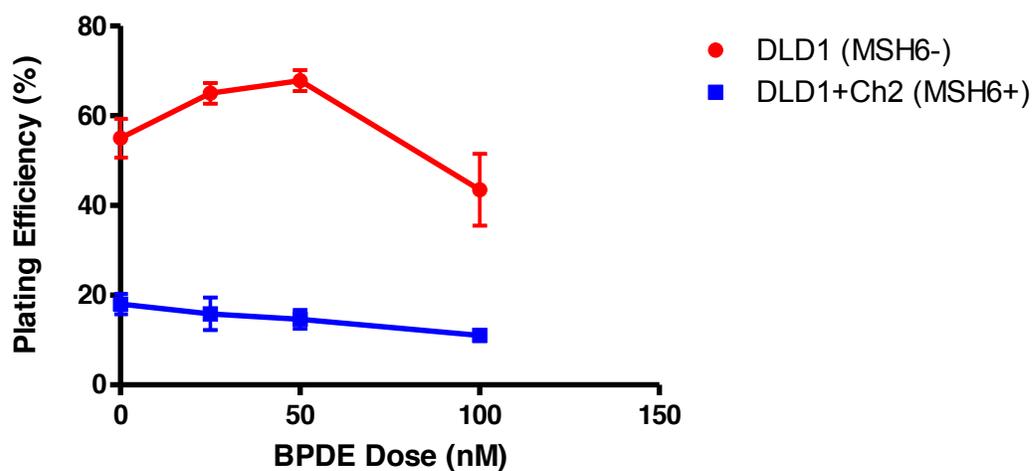
Figure 8. DLD1 and DLD1+Ch2 Plating Efficiency. Plotted are 2 data points at each dose. 300 cells were plated in each plate and plating efficiencies were measured as described in materials and methods

The potential technical issue with plating efficiencies, the fact that the experiment was performed only once, and the unexpected finding make it difficult to draw firm conclusions. It is possible that the high induced mutant frequencies calculated for the

DLD1+Ch2 cell line are not representative of true mutation rates upon exposure to

BPDE. It is also possible that the cell lines might have been switched accidently. Thus

comparisons between the DLD1 and DLD1+Ch2 cell lines are premature at this time.

Lysates of individual DLD1+Ch2 6-TG^R clones from this particular experiment are

available. A western blot should be performed to quantify MSH6 protein levels to

determine whether the cell lines are properly identified. After confirming the identity of

the cell lines, this experiment should be repeated. Additionally, better measurement of

plating efficiencies by allowing colonies to develop longer would result in more robust

calculations of mutant frequencies. If the identity of the MSH6-deficient DLD1 cells is

confirmed, the relatively low rate of BPDE-induced mutation (similar to that of the

MMR-proficient HCT 116+Ch3 cells) is interesting. This low rate of induced mutation

may be the result of redundancy in function in MutS heterodimers. The MutSβ

heterodimeric complex composed of MSH2 and MSH3 proteins may have partial

redundancy with respect to B[A]P -guanine adducts and fill in when MutSα is not

functional.

II. *HAT Plating Efficiency and Mutant Frequency*

HAT (Hypoxanthine-Aminopterin-Thymidine) medium is used in mutagenesis

assays for negative selection against HPRT mutants. Aminopterin blocks de novo

synthesis of purines by acting as a folate metabolism inhibitor, effectively inhibiting

dihydrofolate reductase. For cell division to continue, cells are required to utilize the

salvage pathway by metabolism of hypoxanthine and thymidine. Cells possessing active

HPRT are able to utilize the salvage pathway and synthesize purines and pyrimidines

from intermediates in the degradative pathway for nucleotides (Figure 9). Cells lacking,

or deficient for HPRT cannot rely on the salvage pathway, and will therefore die when

cultured in HAT medium. In HPRT mutagenesis assays, cells are initially grown for a

number of replication cycles in HAT medium to clear the culture of any preexisting

HPRT-mutants.
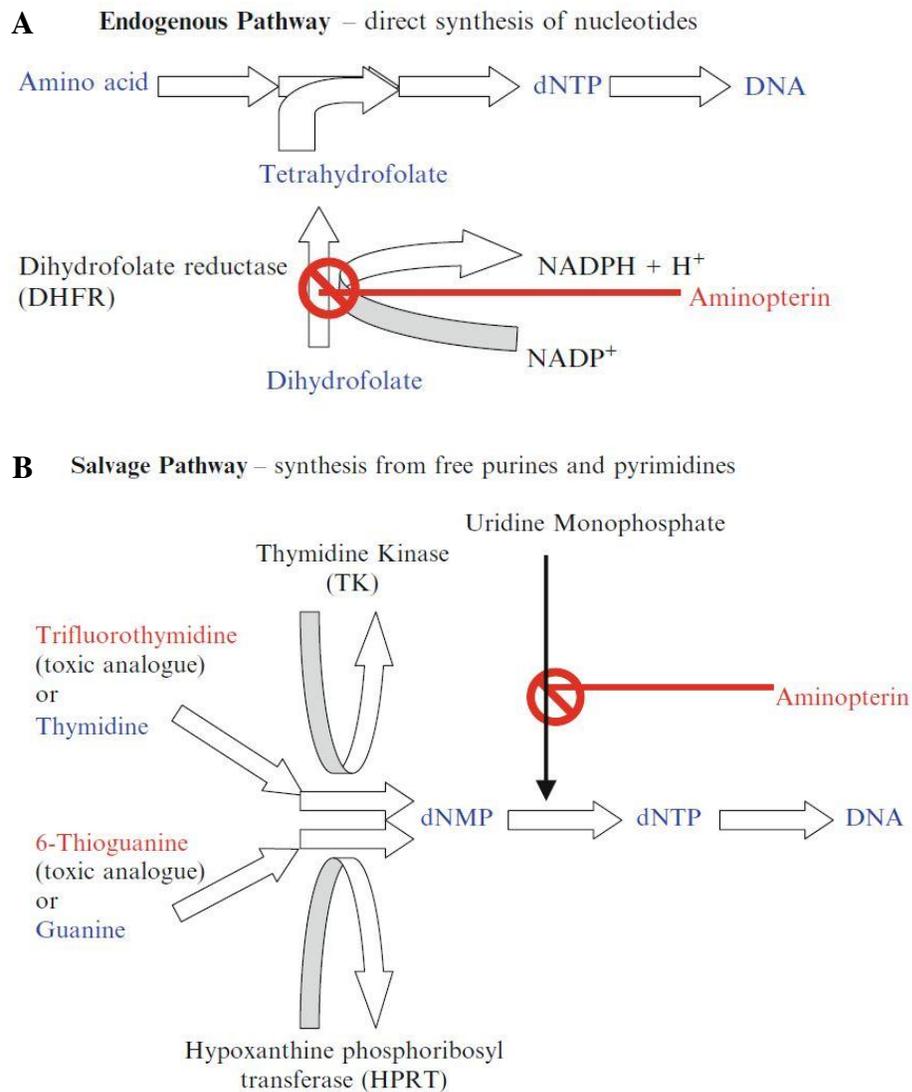
Figure 9. Illustration of endogenous (A) and salvage pathways (B) in the production of dNTPs for DNA synthesis. Aminopterin blocks the synthesis of DNA by inhibiting dihydrofolate reductase. Cells that lack the ability to utilize the salvage pathway for nucleotide synthesis are eliminated. Cells that possess hypoxanthine-guanine phosporibosyl transferase (HPRTase) enzymes can utilize the salvage pathway if supplied with hypoxanthine and thymidine. (Figure from Johnson, 2012).

The high level of spontaneous mutation in initial experiments with the HCT 116

cell line (Figure 5) suggested that HAT treatment may not be working effectively. To

determine the minimum number of population doublings needed in HAT medium to

effectively reduce the frequency of preexisting HPRT mutants in the culture to acceptable

levels, I plated cells in 6-TG after successive passages in HAT medium, and measured

the frequency of 6-TG^R clones (Figure 10). We also tested HCT 116 cells, provided by

two different laboratories to control for any differences that might accumulate randomly

due to growth of these mutator cell lines (Figure 10).

A

B
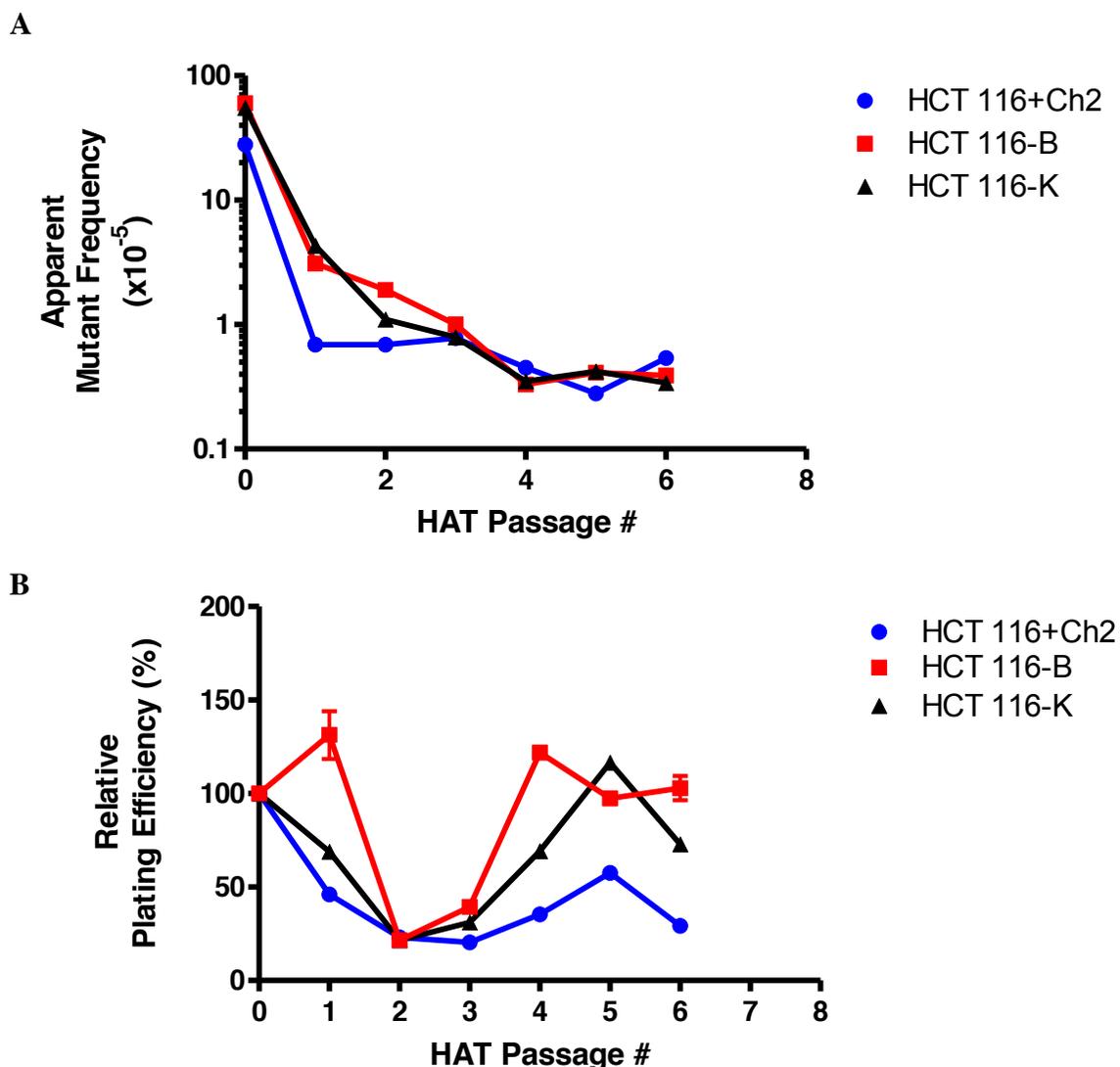
Figure 10. HPRT mutant frequencies following growth in HAT medium (A) and plating efficiencies (B). After five passages in HAT medium, the frequency of mutants was reduced below detectable levels, $\leq$ 0.37 x 10^{-5} mutants. Values after passage 2 in HAT medium are maximum possible values based on plating efficiencies (limit of detection) (A). An initial HAT passage experiment exhibited plating efficiencies that varied dramatically (B). Plating efficiencies were normalized based on absolute plating efficiencies of 58.2% (HCT 116+Ch2), 37.7% (HCT-K) and 23% (HCT-B) at HAT passage #0.

In all cell lines, mutant frequencies decreased significantly after one passage in HAT medium. After five passages in HAT medium, the frequency of preexisting mutants was reduced below detectable levels, approximately ≤ 0.37 x 10^{-5} mutants. Only 1 mutant clone was detected following two passages in HAT medium. Our limit of

detection was based on plating four plates for each cell line at cell densities of 0.135 x

10^6 per plate. With an average plating efficiency of 8.8%, roughly 1.4 x 10^5 live cells

(11,880 x 12 plates) were plated after HAT passage 2 and only 1 HPRT mutant was

detected. After passage 5; however, plating efficiencies were higher, resulting in 5.4 x

10^5 live cells (44,820 x 12 plates) cells and a limit of detection of approximately ≤ 0.37 x

10^{-5} mutants. A similar study with more plates would further reduce the limit of

detection; however, we can confidently say that HAT treatment is effectively clearing

preexisting HPRT mutants and five 1:5 passages was sufficient.

Plating efficiencies and the size of colonies formed in this particular experiment

varied dramatically. As a general trend, it appeared that plating efficiencies initially

decreased but recovered by passage five (based on absolute plating efficiencies of 58%

(HCT 116+Ch2), 38% (HCT-K) and 23% (HCT-B) at HAT passage #0). It is possible

that the initial apparent reduction was a result of technical issues (such as insufficient

time for colony growth) or a true effect of growth in HAT medium.

To determine whether growth in HAT medium affected plating efficiency, I

maintained HCT 116+Ch2 and HCT 116+Ch3 cell lines in HAT and normal IMDM

media in parallel, plating after each passage to determine plating efficiencies.

Subculturing was performed so that all cultures underwent approximately the same

number of replication cycles per passage. I also increased the colony development time

from 8 to 12 days to allow for more robust and easier to count colonies. Results are

shown on following page (Figure 11).

A
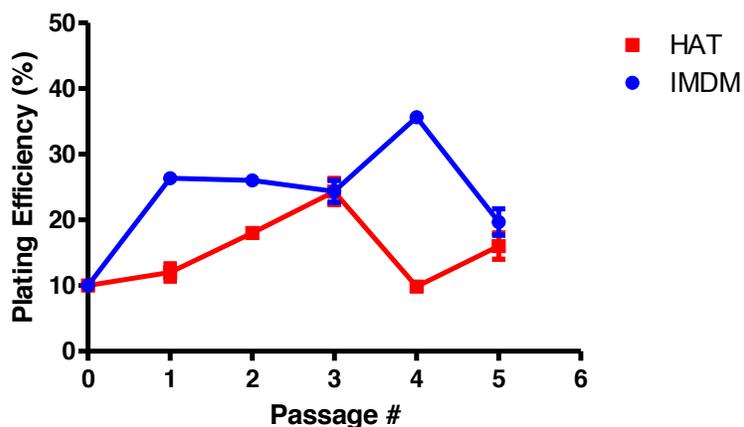
B
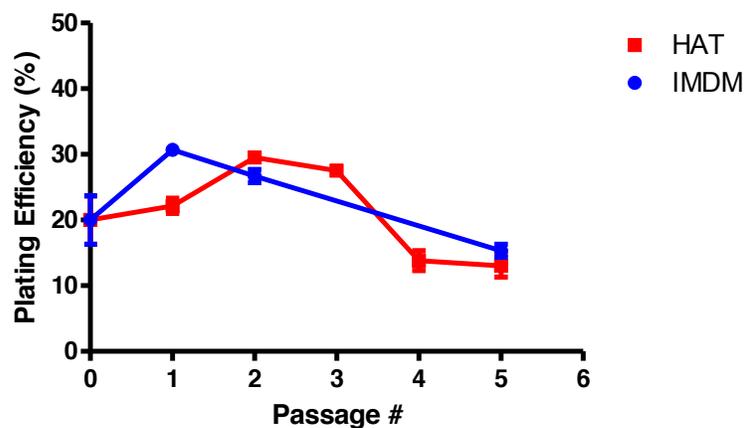
Figure 11. Plating efficiencies following serial passage in HAT and IMDM medium. HCT 116+Ch2 (A) and HCT 116+Ch3 (B) cells were serially cultured in parallel in HAT and IMDM medium. 300 cells were plated in each plate and plating efficiencies were measured as described in materials and methods.

The results from this experiment suggest that the plating efficiency of cells grown in HAT medium was not significantly different than cells grown in the typical IMDM medium (Figure 11). The plating efficiency in the HCT 116+Ch3 cell line decreased approximately by half during 6 consecutive HAT passages while the HCT 116+Ch2 cell line exhibited higher plating efficiencies. The data set for the HCT 116+Ch3 line is missing some critical time points due to the culture growing more slowly and not being

ready for passage. Variation in plating efficiencies over the course of the experiment appears apparent and larger than any differences due to the different types of medium used. Such variation may derive from error introduced during the handling of the cells. It's possible that cell viability was affected during the manual counting of cells or during the preparation of dilutions. We can conclude that the different medium does not significantly affect cell viability. Allowing longer times for colony formation significantly helped achieve a more accurate counting of colonies.

III. BPDE-Induced Mutation: Effect of Source of HCT 116 and Phenotypic Expression Times

Using the HCT 116+Ch2 cell line and two HCT 116 cell lines from different sources (Bolland and Kunkel laboratories), we once again tested our hypothesis to determine whether source of cell line had an impact on the rate of BPDE-induced mutation (Figure 12). With an expectation that excessive replication cycles during the phenotypic expression period would result in elevated spontaneous mutation frequencies, we monitored population doublings following BPDE exposure by visual inspection of cell densities at each passage. Our intent was to determine whether MLH1 status has an effect on BPDE-induced mutation rates. Cultures were exposed to BPDE in parallel and plated into 6-thioguanine after each independent culture had undergone roughly the same number of population doublings throughout the phenotypic expression window of 8 days.

A
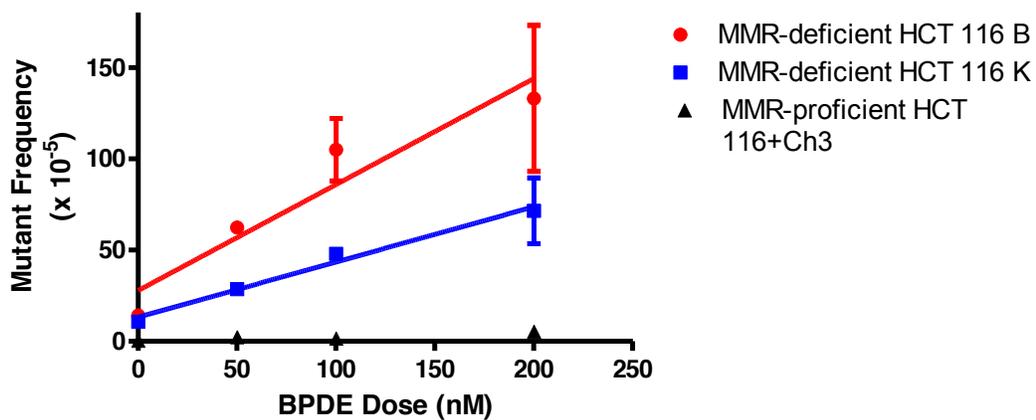
B
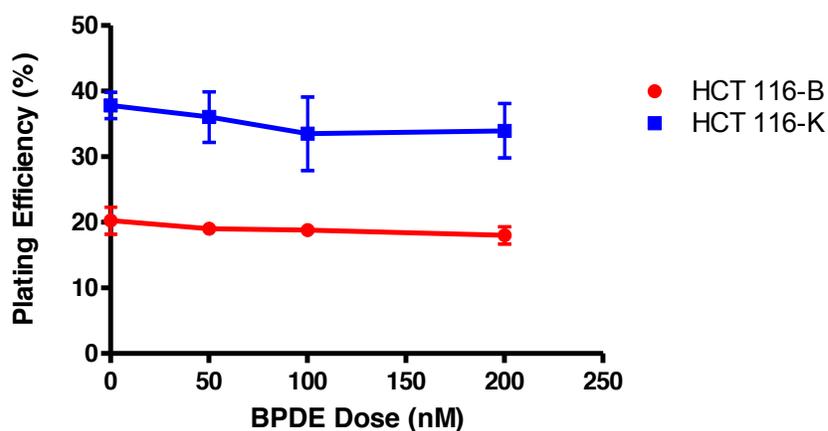
C
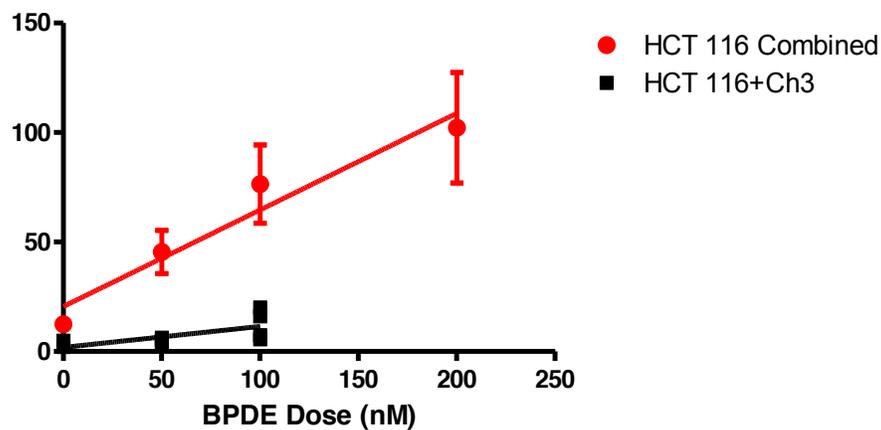
Figure 12. BPDE-induced 6-TG^R mutation rates for HCT 116-B, HCT 116-K and HCT 116+Ch3 cell lines with linear regression shown (A), plating efficiencies for HCT 116-B and HCT 116-K cells (B) and HCT 116 combined BPDE-induced 6-TG^R mutant frequency versus HCT 116+Ch3 cells with linear regression shown (C).

Both cell lines showed lower spontaneous mutation frequencies similar to the preliminary data in the Buermeyer laboratory with the MLH1-deficient HCT 116+Ch2 cells (Figure 4). Based on linear regression analysis, BPDE-induced mutation rates in this experiment for HCT 116-K cells (30±5 mutations per 100 nM BPDE; $r^2 = 0.86$) and for HCT 116-B cells (58±7 mutations per 100 nM BPDE; $r^2 = 0.81$) were not significantly different (p=0.09). We therefore pooled the data for these different cell lines for comparisons with other cell lines, generating a combined BPDE-induced mutation rate (44±10 mutations per 100 nM BPDE; $r^2 = 0.55$) (Figure 12). The HCT 116 combined data set was not significantly different from the HCT 116+Ch2 cells (p=0.51). Both the HCT 116-combined and HCT 116+Ch2 cell lines were significantly different than previously measured HCT 116+Ch3 cells.

Plating efficiency remained relatively constant for different doses of BPDE, but plating efficiencies for the Kunkel sourced HCT 116 cell line appeared lower, approximately half that of the Boland sourced HCT 116 cells. Colonies were small and in some cases difficult to count. It is possible that plating efficiencies were underestimated as small colonies were not counted. This low plating efficiency, when incorporated into the mutant frequency calculation, ultimately increases the mutant frequency, and may partially explain some of the variation in the calculated mutant frequencies.

To observe the effects of extending the phenotypic expression period, HCT 116+Ch2 cells were cleansed with HAT, exposed to BPDE and allowed 7 or 10 days of phenotypic expression before being plated into 6-thiouguanine (Figure 13).

A
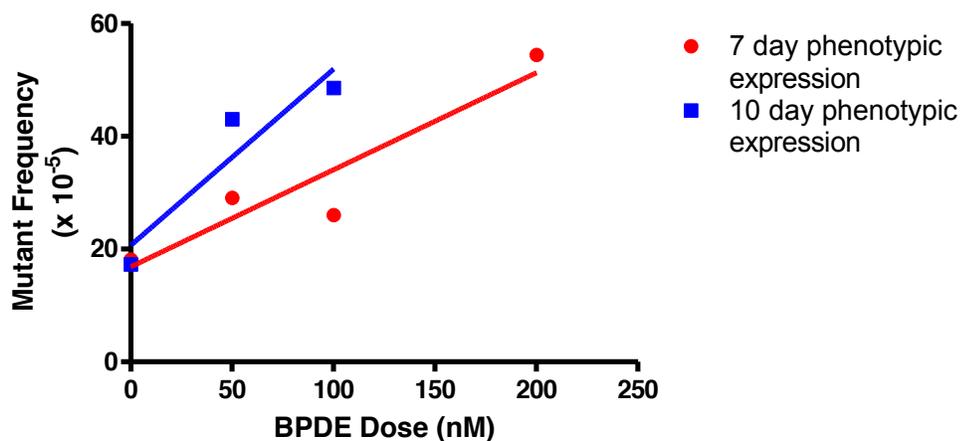
B
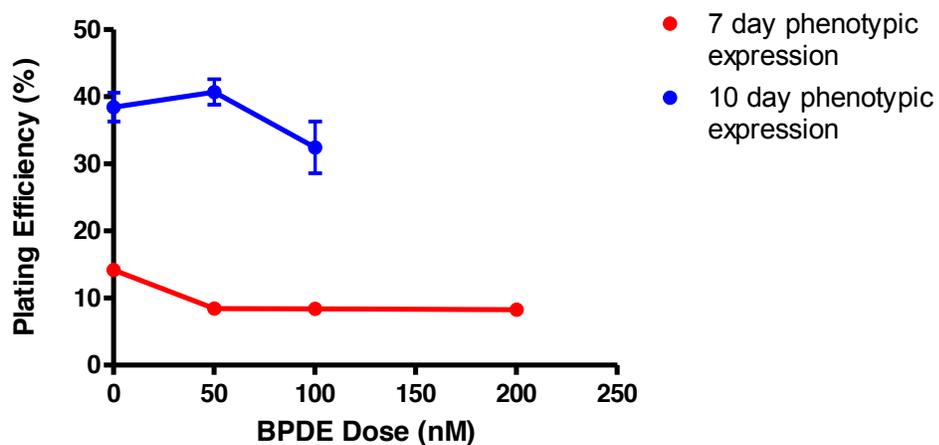
Figure 13. BPDE-induced 6-TG^R mutation rates in MLH1-deficient HCT 116+Ch2 cell lines (A) and corresponding plating efficiencies (B) for 7 and 10 day phenotypic expression windows. Plotted is the linear regression of data from 7 day phenotypic expression (17±6 mutants per 100 nM BPDE; $r^2 = 0.56$) and 10 day phenotypic expression (31±7 mutants per 100 nM BPDE; $r^2 = 0.82$) (p = 0.28).

In this experiment, cell lines experiencing both 7 and 10 days of phenotypic expression exhibited a somewhat higher than expected spontaneous mutation frequencies. The rates of BPDE-induced mutation in cells given 7 days of phenotypic expression was 17±6 mutations per 100 nM BPDE ($r^2 = 0.56$), and 31±7 mutations per 100 nM BPDE in

cells with 10 days of phenotypic expression (Figure 13). These BPDE-induced mutation rates between 7 and 10 days of phenotypic expression time are not significantly different (p=0.28). Plating efficiency was poor in the cells given only 7 days of phenotypic expression. Although extending the phenotypic expression time period by 3 additional days did not have a significant effect on the spontaneous mutant frequency, there is a slight increase in induced mutant frequencies as apparent by the slope of the graph. It was estimated that the 7 and 10 days of phenotypic expression time corresponded to 6 and 10 doublings, based on visual observation of confluency. The 200 nM BPDE dose cultures were passaged separately as confluency was much less than the 0, 50 and 100 nM BPDE dose cultures. The number of population doublings is difficult to accurately determine due to potential cytotoxicity after exposure to BPDE. This was most apparent in the 200 nM BPDE dose. Cell counts rather than visualizing confluency would be a more accurate way to determine the number of population doublings. Once again this experiment shows how important it is to obtain plating efficiencies that are believable, as the plating efficiency has a significant impact on the calculated mutant frequency. Had the plating efficiencies for the culture that experienced a 7 day phenotypic expression period been higher, the corresponding mutant frequencies would have been significantly lower. Our confidence in these data is therefore limited by the low apparent plating efficiency and higher than normal frequency of spontaneous mutation. Rates of induced mutation in the cells given 10 days of phenotypic expression (31 ± 7 mutations per 100 nM BPDE) do resemble the induction in previous experiments using the same cell line (HCT 116+Ch2 induction 30 ± 7 mutations per 100 nM BPDE).

Benzo[a]pyrene + S9 Induced Mutant Frequency

Humans are rarely exposed to single environmental carcinogens. Everyday exposure generally involves complex mixtures of carcinogens. With the intent to study MMR-dependent suppression of genotoxicity posed by complex environmental mixtures, we first need to optimize an assay that has the ability to metabolize these complex mixtures. Most mammalian cell lines, with the exception of those derived from liver cell, lack the ability to metabolize precarcinogens into their genotoxic metabolites and require either exogenous metabolizing mixes or genetic manipulation to induce the expression of metabolizing enzymes. Previous studies in literature describe use of homogenized rat liver, so-called S9 extract, to provide an exogenous source of metabolizing enzymes. Prior exposure of rats to CYP-inducing compounds leads to increased levels of metabolizing enzymes in rat liver S9 extracts. Using B[A]P and an S9 fraction from Aroclor-1254-induced Sprague-Dawley rats, our goal was to establish conditions for measurement of induced mutation with B[A]P and other PAHs, including complex mixtures. Detectable induced mutant frequencies would indicate that the S9 mix has metabolized the B[A]P equivalent to generate BPDE and ultimately B[A]P DNA adducts.

A
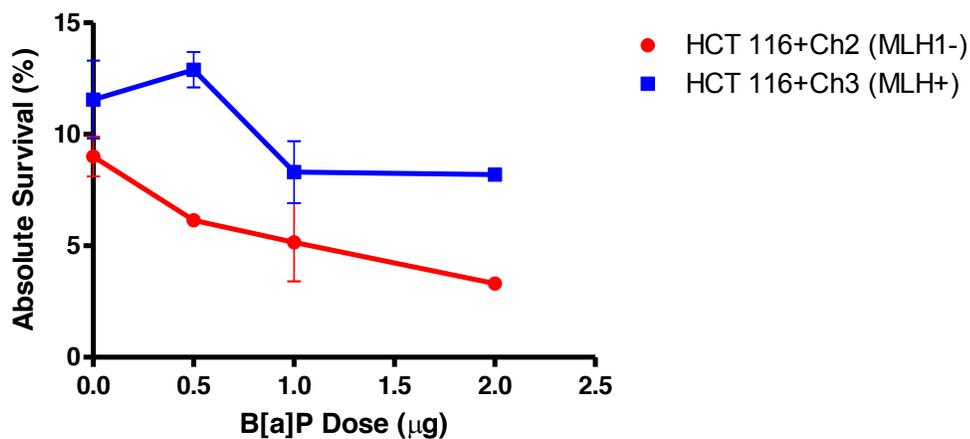
B
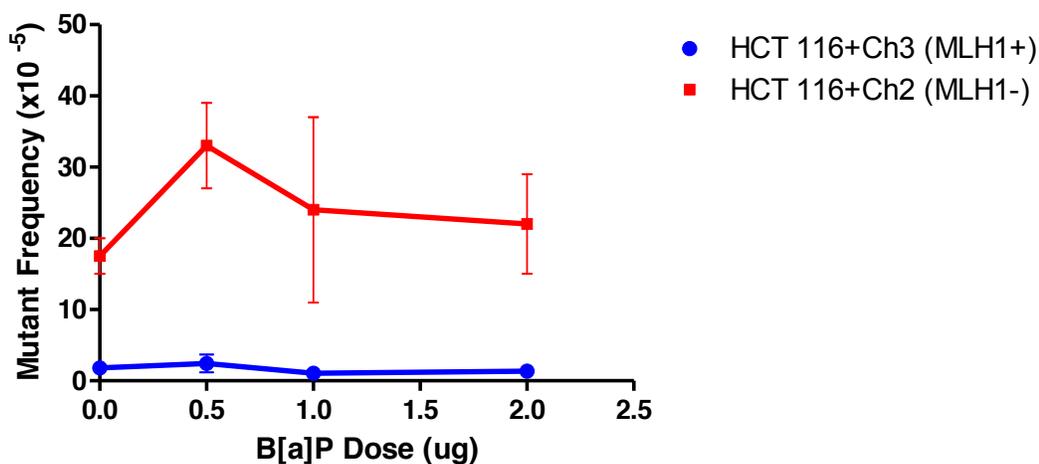
Figure 14. B[a]P + S9 mix cytotoxicity (A) and B[a]P mutant frequency (B) in HCT 116+Ch2 and HCT 116+Ch3 cell lines.

To measure mutations induced by B[a]P, I exposed cells to B[a]P in the presence of a 10% S9 mix as described in the materials and methods. In an initial experiment, plating efficiencies were low (Figure 14A) and decreased slightly with increasing dose of B[a]P. The very low PE even in the absence of B[a]P suggests that the S9 mix was cytotoxic to the cells, even at the zero doses (Figure 14A). Next time this experiment is

performed, a set of plates without S9 mix would be needed to confirm relative plating efficiencies. There was no measurable induction of mutation with any dose of B[a]P. Therefore, it is apparent that when using liver S9 in the mammalian cell gene mutation test, it is important to optimize the concentration of S9 extract for the particular cell line being used. For future studies, different concentrations of S9 would be needed to first optimize the assay, before 6-TG^R clones could be analyzed. A finding of similar mutations induced by metabolically activated B[A]P verse BPDE clones would indicate that the metabolizing environment was producing BPDE that generated mutations. Measurement of DNA adducts could also prove valuable in optimizing conditions for the assay. The results indicate that caution is necessary to investigate the mutagenicity of precarcinogens using S9 to achieve metabolic activation. Once conditions were established for efficient induction of mutation, the use of complex carcinogenic mixtures could be studied.

Characterization of HPRT mutants

To determine the nature of the spontaneous and BPDE induced mutations in the *HPRT* gene, 25 independent 6-TG^R clones were isolated from solvent and BPDE-exposed HCT 116+Ch2 cells. We purified RNA from each clone and analyzed the sequence of the *HPRT* gene by using reverse transcription coupled to PCR amplification and sequencing of the resultant full length *HPRT* coding sequence. The identified mutations are listed in Table 1.

Dose	Position	Exon	Type of Mutation	Amino Acid Change
0	213G	3	insertion	frameshift
0	213G	3	insertion	frameshift
0	A499del	7	deletion	frameshift
50	G88T	2	substitution	STOP
50	G134A	3	substitution	Arg → Lys
50	G135T	3	substitution	Gly → X
50	G211T	3	substitution	Gly → Cys
50	G238T	3	substitution	Asp → Tyr
50	C454T	6	substitution	Gln → Stop
50	G580T	8	substitution	Asp → Tyr
50	T623G	9	substitution	Ile → Ser
50	TG633/634CT	9	substitution	Gly → Trp
50	636G	9	insertion	frameshift
100	TG170/171AT	3	substitution	Met → Asn
100	G419T	6	substitution	Gly → Val
100	G419T	6	substitution	Gly → Val
100	G419T	6	substitution	Gly → Val
100	G569T	8	substitution	Gly → Val
100	A611G	9	substitution	His → Arg
200	11del	1	deletion	frameshift
200	G172T	3	substitution	Gly → Stop
200	G202C	3	substitution	Arg → Pro
200	G403T	6	substitution	Asp → Tyr
200	596G	9	insertion	frameshift
200	G618T	9	substitution	frameshift

Table 2. Identified Spontaneous and BPDE-induced Mutations.

Only 3 mutants from the 0 nM BPDE dose were characterized, 2 were insertions and 1 was a deletion, likely consistent with previous reports in the literature demonstrating a high level of frameshifts, specifically an insertion or deletion of a single base among spontaneous mutations. Of the BPDE-exposed clones, 19 exhibited a base substitution, 14 of which were G·C→T·A transversions, consistent with adduction of B[a]P predominantly to guanine bases. Of the remaining mutants characterized, four

contained an insertion of a single guanine base and two contained a deletion. Mutations

identified in 50, 100 and 200 nm BPDE doses ranged throughout the entire *HPRT* gene.

Although not incorporated into Table 1, four additional clones exhibited sequences with

multiple cDNA products, likely a result of aberrant RNA splicing of the expressed *HPRT*

gene. This preliminary analysis also identified potential hot spots at two sites: an

insertion of guanine at site 213 and a G→T transversion at site 419. We have not started

analysis of BPDE-induced mutations in MLH1-proficient HCT 116+Ch3 cells.

Additional analyses are needed to identify any potential differences in the spectrum of

mutations induced in MMR-proficient versus deficient cells.

Summary of Conclusions and Future Direction

Mammalian cell *HPRT* gene mutation assay can be a sensitive, efficient assay for

measuring the impact of environmental and genetic factors, providing biomarkers of

cancer risk, such as induced mutations. However a number of factors can affect the

observed mutant frequencies. Obtaining reliable plating efficiencies and keeping track of

population doublings during the phenotypic expression period are both important in

producing reproducible, high quality data. A larger-scale study in the future, focused on

identifying the number of population doublings necessary and sufficient for phenotypic

expression, would be valuable. In mutator cell lines this window is apparently narrow,

and if phenotypic expression exceeds the threshold or limit of detection, spontaneous

mutations soon override induced mutation. This has implications for characterization of

the spectrum of mutations that are truly induced.

While a number of technical issues arose throughout the study, slight changes and optimization of the assay led to findings that will be useful for further studies. Plating efficiencies were generally low; however, allowing colonies to develop for 10-12 days rather than 8 made for easier counting and a more reliable measurement of colony-forming ability. In addition, monitoring the number of population doublings or replication cycles is important and variation in doublings among independent cultures should be minimized. The parent HCT 116 cell line demonstrated a BPDE-induced mutation rate of 44±10 mutations per 100 nM BPDE, similar to that of the HCT 116+Ch2 cell lines (30±7 mutations per 100 nM BPDE). We conclude.

For analysis of BPDE-induced mutations, additional clones that an MLH1 role in suppressing mutation is generalizable to the parent cell line, HCT 116. Further studies would be needed to make the same conclusion about the role of other MMR proteins would need to be analyzed before making conclusion about the spectra of mutations induced. However, the preliminary data generally matches that of previously characterized BPDE-induced mutants in published literature. Before studying the effects of mutation induced by complex carcinogenic mixtures, S9 metabolizing conditions will need to be optimized. A study with complex carcinogenic mixtures would give a more valuable and realistic interpretation of the synergistic, additive or deleterious effects that mixtures of PAH's pose to human health and carcinogenesis.

Bibliography

Anyakora, Chimezie, Anthony Ogbeche, Pete Palmer, Herbert Coker. 2005. Determination of polynuclear aromatic hydrocarbons in marine samples of Siokolo fishing settlement. *Journal of Chromatography A*, vol 1073, 323-330.

Baird, William M., Louisa A. Hooven, Brinda Mahadevan. 2005. Carcinogenic Polycyclic Aromatic Hydrocarbon-DNA Adducts and Mechanism of Action. *Environmental and Molecular Mutagenesis*, vol 45, 106-114.

Bostrom, Carl E., Gerde Per, Hanberg Annika. 2002. Cancer Risk Assessment, Indicators, and Guidelines for Polycyclic Aromatic Hydrocarbons in the Ambient Air. *Environmental Health Perspectives*, vol 110, 451-488.

Bostrom, Carl-Elis, Per Gerde, Annika Hanberg, Bengt Jernstrom Christer Johansson, Titus Kyrklund, Agneta Rannug Margareta Tornqvist, KAtarina Victorin, Roger, Westerholm. 2002. Cancer Risk Assessment, Indicators, and Guidelines for Polycyclic Aromatic Hydrocarbons in the Ambient Air. *Environmental Health Perspectives*, vol 110, 451-488.

Cannavo, Elda, Giancarlo Marra, Jacob Sabates-Bellver, Mirco Menigatti, Steven M. Lipkin, Franziska Fischer, Petr Cejka, Josef Jiricny. 2005. Expression of the MutL homologue hMLH3 in human cells and its role in DNA mismatch repair. Cancer Research vol 65,10759-66.

Gabrieli, Jacopo, , Paul Vallelonga, Giulio Cozzi, Paolo Gabrielli, Andrea Gambaro, Michael Sigl, Fabio Decet, Margit Schwikowski, Heinz Gäggeler, Claude Boutron, Paolo Cescon, and Carlo Barbante. 2010. Post 17th-Century Changes of European PAH Emissions Recorded in High-Altitude Alpine Snow and Ice. *Environmental Science & Technology*, vol 44, 3260-3266.

Fukui, Kenji. 2010. DNA Mismatch Repair in Eukaryotes and Bacteria. *Journal of Nucleic Acids*, vol 2010, 1-16.

Jiricny, J. 2006. The Multifaceted mismatch-repair system. *Nature Reviews Molecular Cell Biology*, vol 7, 335-346.

Johnson, George. 2012. Mammalian cell *HPRT* gene mutation assay: test methods. *Methods Mol Biol*. Vol 817, 55-67.

Karttunen, Vesa, Paivi Myllynen, Gabriela Prochazka, Olavi Pelkonen, Dan Segerback, Kirsi Vahakangas. 2010. Placental transfer and DNA binding of benzo[a]pyrene in human placental perfusion. *Toxicology Letters*, vol 197, 75-81.

K.W. Kinzler, B. Vogelstein. 1996. Lessons from hereditary colorectal cancer. *Cell*, vol 87, 159-170.

Lagerquist, Anne, Daniel Hakansson, Gabriela Prochazka, Cecilia Lundin, Kristian Dreij, Dan Segerback, Bengt Jernstrom,Margareta Tornqvist, Albrecht Seidel, Klaus Erixon, Dag Jenssen. 2008. Both replication bypass fidelity and repair efficiency influence the yield of mutations per target dose in intact mammalian cells induced by benzo[a]pyrene-diol-epoxide and bibenzo[a,l]pyrene-diol-epoxide. *DNA Repair,* vol 7, 1202-1212.

Loeb, Lawrence. 2011. Human cancers express mutator phenotypes: origin, consequences and targeting. *Nature Reviews Cancer,* vol 11, 450-457.

Phillips, David H. 1999. Polycyclic aromatic hydrocarbons in the diet. *Mutation Research*, vol 443, 139-147.

Pino, Maria, Mari Mino-Kenudson, Bernadette Mandes Wildemore, Aniruddha Ganguly, Julie Batten,Isabella Sperduti, Anthony John Iafrate, Daniel C. Chung. 2009. Deficient DNA MMR Is common in Lynch Syndrome-associated colorectal adenomas. *Journal of Molecular Diagnostics,* vol 11, 238–247.

Ravindra, Khaiwal., Sokhi, Ranjeet. 2007. Atmospheric polycyclic aromatic hydrocarbons: Source attribution, emission factors and regulation. *Atmospheric Environment*, 2-31.

Shimada, T. 2006. Xenobiotic-metabolizing enzymes involved in activation and detoxification of carcinogenic polycyclic aromatic hydrocarbons. *Drug Metabolic Pharmacokinetics*, Vol 21, 257-276, 1347-4367 (Print)

Tarantini, Adeline, Anne Maitre Emmanuel Lefebvre, Marie Marques, Caroline Marie, Jean-Luc Ravanat, Thierry Douki. 2009. Relative contribution of DNA strand breaks and DNA adducts to the genotoxicity of benzo[a]pyrene as a pure compound and in complex mixtures. *Mutation Research*, vol 671, 67-75.

Thakker, D.R., Levin, W., Wood, A. W., Conney, A.H., Yagi, H., Jerina, D.M. 1988. Stereoselective biotransformation of polycyclical aromatic hydrocarbons to ultimate carcinogens. *Stereoselective Aspects of Pharmacologically Actice Compounds*,271–296.

Wang, Jean, Winfried Edelmann. 2006. Mismatch Repair proteins as sensors of alkylation DNA damage. *Cancer Cell*, vol 9, 417-418.

Wu, Jianxin, Liya Gu, Huixian Wang, Nicholas E. Geacintov, Guo-Min Li. 1999. Mismatch Repair Processing of Carcinogen-DNA Adducts Triggers Apoptosis. Molecular and Cellular Biology 19 (12), 8292-8301.

Zhang, Yanxu, Shu Tao. 2009. Global atmospheric emission inventory of polycyclic aromatic hydrocarbons (PAHs) for 2004. *Atmospheric Environment*, vol 43, 812-819.